Saline-enhanced Radiofrequency Thermal Ablation: Is it associated With Complete Tissue Necrosis within the induced Thermal Lesion?

S. Rafie[1], S. G. Nour[1], M. S. Breen[2], J. Jesberger[1], J. L. Duerk[1,2], J. S. Lewin[1,2], M. Rodgers[3]

[1]Radiology, Case Western Reserve University, Cleveland, Ohio, United States, [2]Biomedical Engineering, Case Western Reserve University, Cleveland, Ohio, United States, [3]Pathology, Case Western Reserve University, Cleveland, Ohio, United States

Introduction:

Percutaneous Radiofrequency (RF) Thermal therapy has gained significant interest as a minimally invasive method of treatment for localized malignancy. However, RF thermal ablation has been limited by the size of tumor necrosis that can be created with a single electrode application[1]. One of the effective techniques that have been advocated to augment the coagulative response of RF thermal therapy is direct adjuvant parenchyma injection of a hypertonic NaCl solution[4]. Previous work has demonstrated the ability of MRI to guide saline injection and to monitor the evolution of the thermal lesion within the wet tissue [3]. It has been demonstrated that the central iso/hypointense area detected on post-ablation MRI scans matches the zone of histological coagulative necrosis [6]. MRI monitoring of saline-enhanced lesions was reported to demonstrate brighter foci within these central iso/hypointensity areas. The nature of these foci has not yet been ascertained. Before applying saline-enhanced thermal ablation therapy in patients', it is vital to ensure that these foci do not represent viable tumor tissue. The aim of this study is to scrutinize the induced saline-enhanced thermal lesions for any evidence of histological inhomogeneity within the boundaries of coagulative necrosis with particular emphasis to the foci with questionable MRI signal characteristics.

Material and Methods:

Using a protocol approved by our institutional animal care and use committee, 16 saline-enhanced thermal ablation procedures were performed in the paraspinal muscles of six rabbits using a 17-gauge titanium electrode with a 1-cm exposed tip (Radionics Inc., Burlington, MA), and a conventional monopolar RF technique. All procedures were performed under IV sedation and were monitored on a 1.5T MR scanner (Sonata, Siemens Medical Solutions, Germany). Ablations were randomly distributed over various paraspinal levels and located about 1cm from midline. One lesion was made on each side of the spine in the first 3 animals, and 2 lesions were made on each side of the spine in the next 3 animals. 2-3 ml of saturated NaCl solution (~ 38.5%) were first injected into the planned ablation site. Subsequently the RF electrode was inserted within the pre-injected muscle. Radiofrequency ablation in all 18 procedures was performed using a 200Watt RF generator (RFG-3C: Radionics Inc., Burlington, MA). All ablations were performed at 90±2°C tip temperature for 10 min. Deposited RF current, power, tissue impedance and electrode tip temperature were recorded at one-minute intervals throughout each ablation procedure. Post ablation MR scanning consisted of TSE T2WI (TR/TE/NSA/ETL= 4000/104/3/7), TSE STIR (TR/TE/NSA/ETL= 5540/57/3/7), and pre and post-gadolinium SE T1WI (TR/TE/NSA/FA =600/19/3/90º). The same pulse sequences were implemented to obtain follow-up MR images immediately before animal sacrifice. Thermal lesions were harvested after six days (n=12). Four lesions were harvested within 24 hours of ablation. Paraspinal muscles harboring 16 thermal lesions were harvested for careful histopathological evaluation. Each lesion was carefully sliced at 3 mm thickness and stained with hematoxylin and eosin (H&E) stain.

Results:

The MRI features of saline-enhanced thermal lesions (Figure 1, a and b) followed the general characteristics of standard lesions: an iso/hypointense central zone surrounded by a hyperintense rim on T2-weighted and STIR images with marginal enhancement demonstrated on post-contrast T1-weighted images. Two features were, however, characteristic of saline-enhanced lesions. First, these lesions demonstrated irregular largely irreproducible morphology as compared to the perfectly ellipsoid appearance expected with the standard ablation technique. Second; saline-enhanced lesions consistently demonstrated ill-defined zones of increased signal intensity on T2-weighted (arrows, b) and STIR images which appeared to be included within the boundaries of the marginally enhancing rim seen on post-contrast T1-weighted scan (arrowheads, a). Histological analysis of thermal lesions (Figure 1, c and d) demonstrated well-demarcated homogeneous areas of coagulation necrosis consisting of distorted muscle architecture with contraction bands and redundant pyknosis, separated from the intact adjacent muscle fibers by a zone of inflammatory cells with no evidence of viable tissue within the coagulated zone.

Discussion:

This investigation addresses the issue of applicability of saline-enhanced radiofrequency thermal ablation in an animal model of the clinical setting. Our initial results point to the ability of this technique to effectively eliminate all viable tissues within the significantly larger thermal lesions, thereby supporting the hypothesis that safe and effective tumor eradication can be achieved utilizing this modified technique. Although larger lesions can be induced by the saline-enhancement technique, the three dimensional morphology of the lesion is less predictable, corroborating prior results. This limitation may be, however, overcome by the use of interventional MRI techniques to guide and monitor saline injection and subsequent ablation.

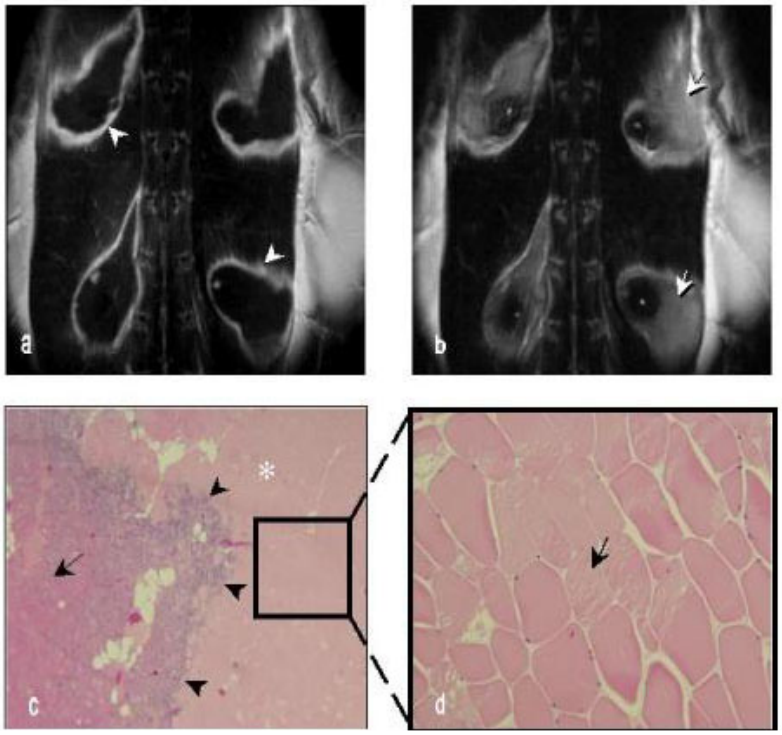

***Figure 1**: Coronal CE-T1WI (a) and Coronal T2WI (b) MRI images acquired 6 days post ablation of the paraspinal muscles showing two lesions on each side of the spine. Note the irregular appearance of thermal lesions that appears to map an uneven saline distribution within the muscles. Also note the ill-defined hyperintense zones on T2WI (arrows, b) that lay within the confinements of the marginally enhancing lesion borders on CE-T1WI (arrowheads, a). 40x (d) and 10x (c) H&E-stained histological sections showing the area of coagulation necrosis (asterisks, c) marginated by a layer of inflammatory cells (arrowheads, c) with well-demarcated inner margin, separating the thermally injured area from the intact muscle fibers (arrow, c). The 40x-magnified section (d) illustrates the featureless coagulated muscle fibers with contraction bands (arrow, d) denoting acute damage and with redundant pyknotic nuclei.*

References:

[1] Goldberg SN, et al. Acad Radiol 1995 ;2:399-404.
[2] Lazebnik RS - *J Magn Reson Imaging* - 01-OCT-2003; 18(4): 487-95
[3] Nour et al. Proceedings of the RSNA 88th Scientific Meeting, 2002, p 218
[4] Goldberg SN, et al. Radiology 2001; 219: 157-165
[5] NourSG,etalRadiology.2002Aug;224(2):452-62.
[6] Breen MS - *J Magn Reson Imaging* - 01-JUL-2003; 18(1): 90-102.
[7] Lewin JS et al. J magn Reson Imaging 1998;8:40-47